

OPTICAL INVESTIGATIONS OF ALTERNATIVE FUEL COMBUSTION IN COMMON RAIL COMPRESSION IGNITION ENGINE

Simona Silvia Merola, Cinzia Tornatore, Gerardo Valentino, Luca Marchitto

*Istituto Motori, National Research Council of Italy
Viale G. Marconi, 4, 80125 Naples, Italy
tel.: +39 081 7177224, +39 081 7177103
+39 081 7177129, +39 081 7177119
e-mail: s.merola@im.cnr.it, c.tornatore@im.cnr.it
g.valentino@im.cnr.it, l.marchitto@im.cnr.it*

Abstract

The increasing global energy demand and the decreasing fossil-energy resources are enhancing the interest in the combustion characteristics of alternative fuels for diesel engines. Alternative-fuel combustion has been studied in detail in light-duty diesel engines, even if the comparison of test results from different chemical nature fuels obtained by integrated optical methodologies is lacking. Thus, it is the primary objective of the present study to characterize the combustion of selected alternative fuels in an optical common rail compression ignition engine by high-speed luminescence imaging and natural emission spectroscopy. The effects of the fuels on in-cylinder spray combustion and soot formation were investigated through UV-visible digital imaging and natural emission spectroscopy. Experiments were performed in a single cylinder high swirl compression ignition engine. The test engine was optically accessible and equipped with a common rail multi-jets injection system. Several injection pressures and timings at two EGR rates were tested. Digital imaging allowed characterizing the evaporating spray and the combustion process. UV-visible emission spectroscopy was used to follow the evolution of the combustion process chemical markers. Chemiluminescence signal due to OH was identified. The soot spectral feature in the visible wavelength range was correlated to soot engine out emissions. Conventional and optical data related to diesel fuel blended with gasoline and butanol were compared.

Keywords: *Optical diagnostics, alternative fuels, diesel fuel, common rail, compression ignition engine*

1. Introduction

The target of a sustainable mobility has led to investigate advanced combustion modes and advanced fuels technologies. Several countries have revised their energy policies and put more and more attention to renewable energy sources. As example, EU has stated that by 2020 at least 10% of the whole fuels used in transport must be renewable. To meet these needs the new generation engines should be optimized for alternative fuels. Literature is too full of works about the outcomes of alternative fuels on the engine performance and emissions. To better understand the effect of the new combustion modes and fuels, detailed studies on the in-cylinder spray and combustion processes are necessary. The optical diagnostics supported by conventional methodologies (such as indicated pressure measurement) are powerful tools for this target [1]. For optical diagnostics, high pressure and temperature constant-volume vessels are useful because they allow high spatial and temporal resolution investigations of the spray; on the other hand, the optical accessible engines permit to simultaneously study fuel injection and combustion phase. Spray engines able to work in conditions very close to real engines and equipped of wide optical accesses often represent the best compromise to obtain valuable information about fuel spray distribution and evaporation, mixture preparation, auto-ignition, spatial distribution of key transient species, and, finally, pollutants formation [2].

Studies on the fuel spray combustion can be classified into two categories: macroscopic and microscopic. The macroscopic analysis of phenomena such as the fuel jet penetration or the flame propagation are optimally investigated by direct visualization methods [3]. Meanwhile, the spray

microscopic parameters such as flow field and droplet size can be measured using either PIV (particle image velocimetry) or PDPA (phase Doppler particle anemometry) [4]. Microscopic characterization of combustion process needs techniques able to detect chemical species or specific compounds such as natural or laser induced emission or extinction spectroscopy.

In this paper, CR diesel processes from fuel injection to exhaust phase were analyzed by combined optical measurements. Several compression ignition combustion modes were investigated through optical diagnostics. Blends of diesel with gasoline and butanol were tested to study the effect of low cetane number.

Butanol has strong potential as a biofuel because it can be produced both by petrochemical and fermentative processes like ethanol [5]. The production of bio-butanol by fermentation offers certain advantages in comparison with bio-ethanol: higher energy content, lower water adsorption and corrosive properties, better blending abilities and the ability to be used in conventional internal combustion engines without the need for modification. Although bio-butanol could not compete on a commercial scale with butanol produced synthetically and almost all production ceased as the petrochemical industry evolved, the increasing interest in use of bio-butanol as a transport fuel has induced a number of companies to explore novel alternatives to traditional ABE fermentation, which would enable bio-butanol to be produced on an industrial scale.

The tested engine conditions were selected in order to realize three combustion regimes: mixing controlled, conventional and premixed low-temperature combustion. The mixing-controlled combustion was investigated in detail because it was able to maintain low PM and NO_x. The test engine was an optically accessible single cylinder high swirl compression ignition engine equipped with a common rail multi-jets injection system. Integrated diagnostics were applied. They included the conventional measurements of pressure signal and engine-out emissions (NO_x and smoke number) and optical investigations based on UV-visible imaging, chemiluminescence and natural emission spectroscopy. UV-visible digital imaging allowed following the combustion process from the autoignition until the late combustion phase. UV-visible emission spectroscopy was used for the detection of the chemical markers of combustion process. OH radiative emissions were correlated to NO measured at the engine exhaust. The soot spectral feature in the visible wavelength range was correlated to soot engine out emissions.

2. Experimental apparatus

The experiments were carried out in an external high swirl optically accessed combustion bowl connected to a single cylinder 2-stroke high pressure common rail compression ignition engine. The main engine specifications are reported in Tab. 1. The external combustion bowl (50 mm in diameter and 30 mm in depth) is suitable to stabilize, at the end of compression stroke, swirl conditions to reproduce the fluid dynamic environment similar to those within a real direct injection diesel engine. The implication of “cylindrical bowl” is related to the peculiar design of the prototype engine that has a large displacement as an air compressor.

The main cylinder, connected to the external “swirled bowl” through a tangential duct, allows supplying compressed air flow to the bowl as the piston approaches TDC. The air flow, coming from the cylinder, is forced within the combustion chamber by means of the tangential duct. In this way, a counter clockwise swirl flow, with the rotation axis about coincident to the symmetry axis of the chamber, is generated.

The injector was mounted within this swirled chamber with its axis coincident to the chamber axis; in this way the fuel, injected by the nozzle, is mixed up through a typical interaction with the swirling air flow. The combustion process starts and mainly proceeds in the chamber. As soon as the piston moves downward, the flow reverses its motion and the hot gases flow through the tangential duct to the cylinder and finally to the exhaust ports. The combustion chamber provides both a circular optical access (50 mm diameter), on one side of it, used to collect images and a rectangular one (size of 10 x 50 mm) at 90°, outlined on the cylindrical surface of the chamber,

used for the laser illumination input. The injection equipment includes a common rail injection system with a solenoid controlled injector located on the opposite side of the circular optical access. The nozzle is a micro-sac 7 hole, 0.141 mm diameter, 148° spray angle nozzle. An external roots blower provided an absolute air pressure at the inlet of 0.21 MPa with a peak pressure within the combustion chamber of 4.9 MPa under motored conditions.

Tab. 1. Specifications of the engine

| 2-stroke single cylinder ci engine | |
|------------------------------------|--------------|
| Cylindrical Bowl (mmxmm) | 50x30 |
| Bore (mm) | 150 |
| Stroke (mm) | 170 |
| Connecting Rod (mm) | 360 |
| Compression ratio | 10.1:1 |
| Air supply | Roots Blower |
| Outlet/Inlet Blower Ratio | 2.1 |
| Bosch Injector nozzle | 7/0.141/148° |

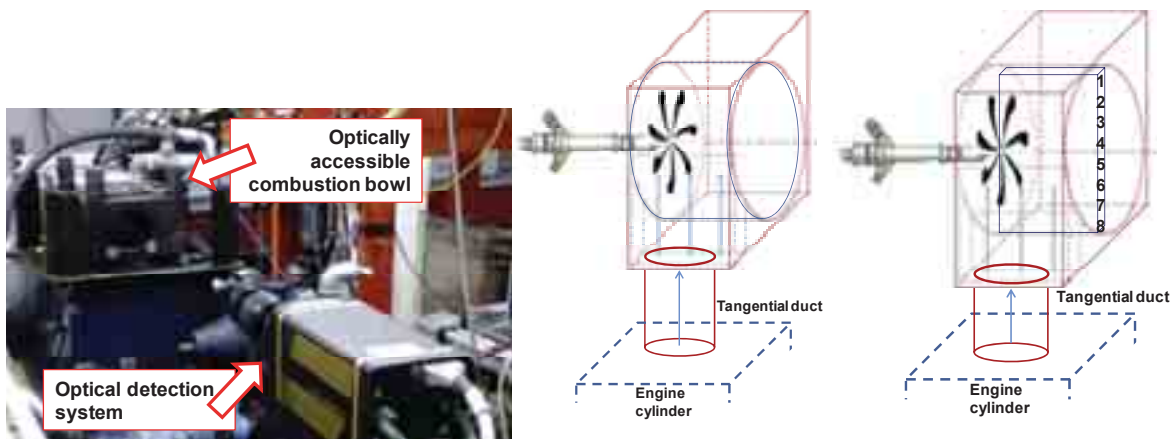


Fig. 1. Pictures of the experimental apparatus for the optical investigations (left) and drawing of injector position in the optically accessible combustion chamber. The regions for the visualization (centre) and for the spectroscopic investigations (right) are marked

In the preliminary phase of the work, spray evolution and combustion process visualization were obtained using an intensified CCD camera (PIMAX - Princeton Instruments) equipped with a quartz lens (UV-Nikon 78-mm), collecting the light emission that passes through the optical access of the combustion chamber. The electronically gated ICCD camera had an array size of 512 x 512 pixels with a pixel size of 19x19 μm and 16-bit dynamic range digitization at 100 kHz. The match between the ICCD and the lens allowed 185 μm spatial resolution. The camera spectral range spread from UV (180 nm) until visible (700 nm). The line-of-sight light emission measurements were performed in the whole ICCD spectral range. The ICCD is not a cycle resolved detector, each acquisition was carried out at a fixed crank angle for different engine cycles setting the exposure time at 5 μs . The temporal difference between two images was 50 μs . For spray visualization, the combustion chamber was back-illuminated by two 250 W halogen lamps in order to visualize the fuel jets before the start of combustion. During the combustion, the lamps were switched off. Pictures and sketches of the experimental apparatus for the optical investigations are reported in Fig. 1.

For spectroscopic investigations, the radiative emissions from the combustion chamber were focused by a 78 mm focal length, f/3.8 UV Nikon objective onto the micrometer controlled entrance slit of a spectrometer (Acton SP2150) with 150 mm focal length and 600 groove/mm grating. From the grating the radiations were detected by an intensified CCD camera (PI-MAX3 - Princeton Instruments). The camera had an array size of 1024 x 1024 pixels with a pixel size of

13x13 μm and 16-bit dynamic range digitization at 100 kHz. The exposure time was fixed at 41.6 μs and the dwell time between two consecutive acquisitions was set at 0.15 CAD \approx 50 μs . The central wavelength of the grating was fixed at 300 nm and 400 nm, respectively, in order to cover the spectral range from UV to visible.

Spectroscopic investigations were carried out in the central region of the combustion chamber. Region of interest for spectroscopic investigation included 512 rows (or spectra) and it was divided in 8 locations. To enhance signal to noise ratio the 64 spectra of each location were averaged. The spectra were corrected for the optical setup efficiency using a deuterium lamp with a highly uniform full spectrum. The wavelength calibration was performed using a mercury lamp. The time evolution of combustion products was evaluated from spectroscopic investigations using a post-processing procedure. For each chemical species with well-resolvable narrow emission bands, the height of the band expressed in counts was evaluated after the subtraction of emission background and other species contribution. Thus OH emission was evaluated as height of the 310 nm band system after the subtraction of the emission background, evaluated as the mean value between the emissions measured at 300 nm and 320 nm. For broadband emission the mean intensity, at specific wavelength range, was considered. Thus, soot emission was evaluated as mean intensity at 530-532 nm. A routine, developed in Labview environment, allowed to simultaneously evaluate the emissions of the selected compounds and species for each spectrum and each time. Moreover, OH and soot emissions were calculated as average on all the spectra.

Tab. 2. Properties of tested fuels

| Fuel Properties | Diesel | G20 | BU20 |
|---------------------------------------|--------|------|-------|
| Density @ 15°C [kg/m ³] | 840 | 835 | 830.4 |
| Viscosity @ 40°C [mm ² /s] | 3.2 | 2.9 | 2.2 |
| Cetane Number | 52 | 44 | 46 |
| Net Heat Value [MJ/kg] | 42.5 | 42.4 | 41.0 |
| Carbon content [%] | 87.0 | 86.8 | 80.2 |
| Hydrogen content [%] | 12.6 | 13.0 | 15.4 |
| Distillation 50% Vol. [°C] | 280 | 250 | 233 |
| Distillation 90% Vol. [°C] | 338 | 328 | 330 |

Optical diagnostics of combustion process were applied considering three fuels. The baseline fuel was the European low sulphur (10 ppm) commercial diesel with a cetane number of 52. Moreover, two blends were tested; the first one was obtained by blending 80% of the baseline diesel and 20% of commercial 98 octane gasoline by volume, denoted as G20 in the following. The second blend was composed by 80% of the baseline diesel and 20% of n-butanol by volume and denoted as BU20. The main properties of the tested fuels are reported in Tab. 2.

In the combustion tests, data were collected using the AVL INDICOM driven by an optical encoder with 0.2 crank angle degree resolution. The pressure within the swirl chamber was acquired by a quartz pressure transducer AVL QC34C and the rate of heat release was computed by the pressure signal, assuming no pressure difference between the swirl chamber and the cylinder. Results of the in-cylinder pressure have been computed averaging 300 consecutive engine cycles. Exhaust gaseous emissions have been acquired by the AVL DiGas 4000 analyzer for NO_x (1 ppm resolution), the Smoke Meter AVL 415S was used for FSN (0.01 resolution) measurements. All combustion tests were carried out running the engine at the fixed speed of 500 rpm, injecting a fuel amount of 30mg \pm 1% at the pressure of 70 MPa. Tests were carried out setting the electronic injection timing (SOI) at 11 CAD BTDC, 3 CAD BTDC, 1 CAD ATDC and 5 CAD ATDC at two EGR rates, 0% and 50% corresponding to oxygen concentration at intake of 21 and 17%, respectively.

3. Results and Discussion

Figure 2 shows the ignition delay evaluated from pressure related data; moving the SOI from 11 CAD BTDC towards later start of injection, a longer ignition delay was observed for all the fuels. This trend is confirmed both at EGR=0 and 50% suggesting that the decrease in the fuel cetane number increases the ignition delay for the low and high temperature conditions.

Pressure signals detected in the combustion chamber for condition with SOI=11 CAD BTDC were featured by moderate higher peaks for G20 and BU20 compared with diesel, both at EGR=0 and 50%. This effect was due to the larger amount of fuel burnt during the premixed combustion because of the increased ignition delay. At SOI=3 CAD BTDC the ignition delay showed a minimum value due to the occurrence of the injection around the TDC. After this time the ignition delay increasing until to the inception of partial premixed low temperature combustion (PPLTC). For BU20 this occurred in correspondence of SOI=5 CAD ATDC and EGR= 50%. G20 achieved the same regime with the same injection strategy even without EGR. For diesel fuel, the low temperature combustion mechanism was not attained in the selected injection conditions.

During PPLTC, the total amount of injected fuel was delivered earlier than the crank angle at which the start of combustion (PSOC) occurred. The consequence of the enhanced mixing pre-combustion was simultaneously NO_x and smoke reduction. This effect is reported in Figures 3 that show the engine out soot (left plot) and NO_x (right plot) emissions versus the start of injection (SOI) for all the operative conditions.

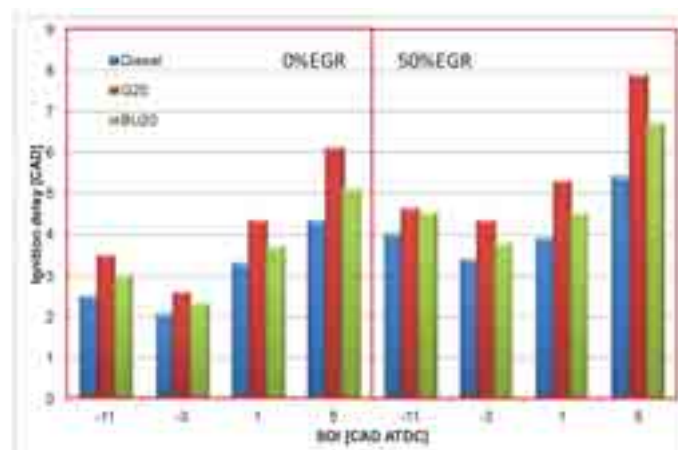


Fig. 2. Ignition delay vs. the start of injection (SOI) for all the operative conditions

In early injection condition (11CAD BTDC), the mixing controlled combustion (MCC) allowed to match the highest working area with very low level of smoke. In particular for BU20 and G20 the soot emission resulted low enough even if high EGR rate was fixed to reduce the level of NO_x to acceptable value. Conventional combustion modes achieved at SOI 3CAD BTDC were characterized by the worst soot-NO_x trade-off. This improved retarding the SOI in particular for BU20. In late injection condition (5 CAD ATDC), the PPLTC mechanism allowed to reduce soot and NO_x emissions close to zero but with penalty for the engine efficiency.

In order to better understand the effect of the different fuels on the evolution of the combustion process, optical investigations are necessary. Fig. 4 shows a selection of images detected in the UV-visible spectral range to follow the spray evolution from the start of injection until autoignition for diesel fuel in the condition with SOI= 1 CAD ATDC and EGR=0%. In all the conditions the fuel coming out from the nozzle proceeds toward the bowl wall interacting with the hot swirling air without interference between the jets that remained well separated. Auto ignition occurred near the tip of the jet and thus it was correlated to the fuel spray penetration.

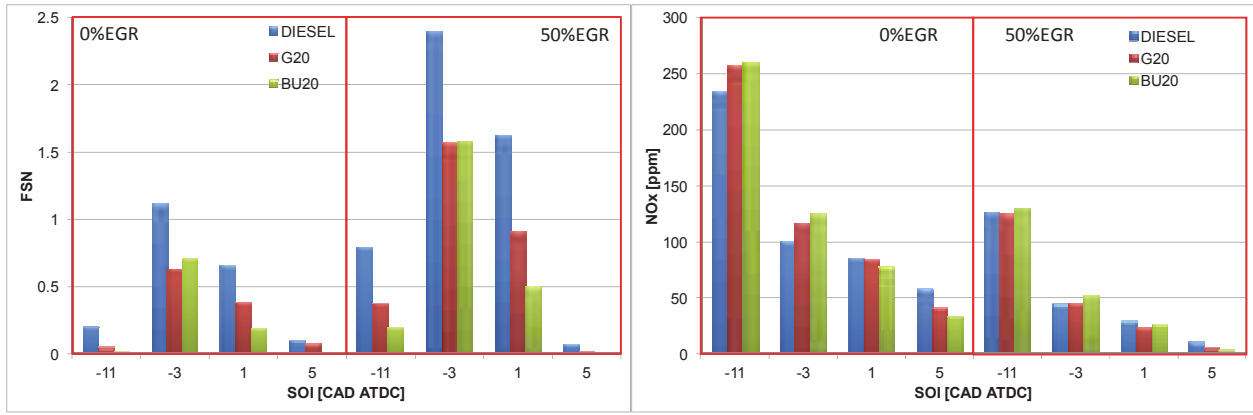


Fig. 3. Engine exhaust emissions of soot (filter smoke number - FSN) and NOx vs. the start of injection (SOI) for all the operative conditions

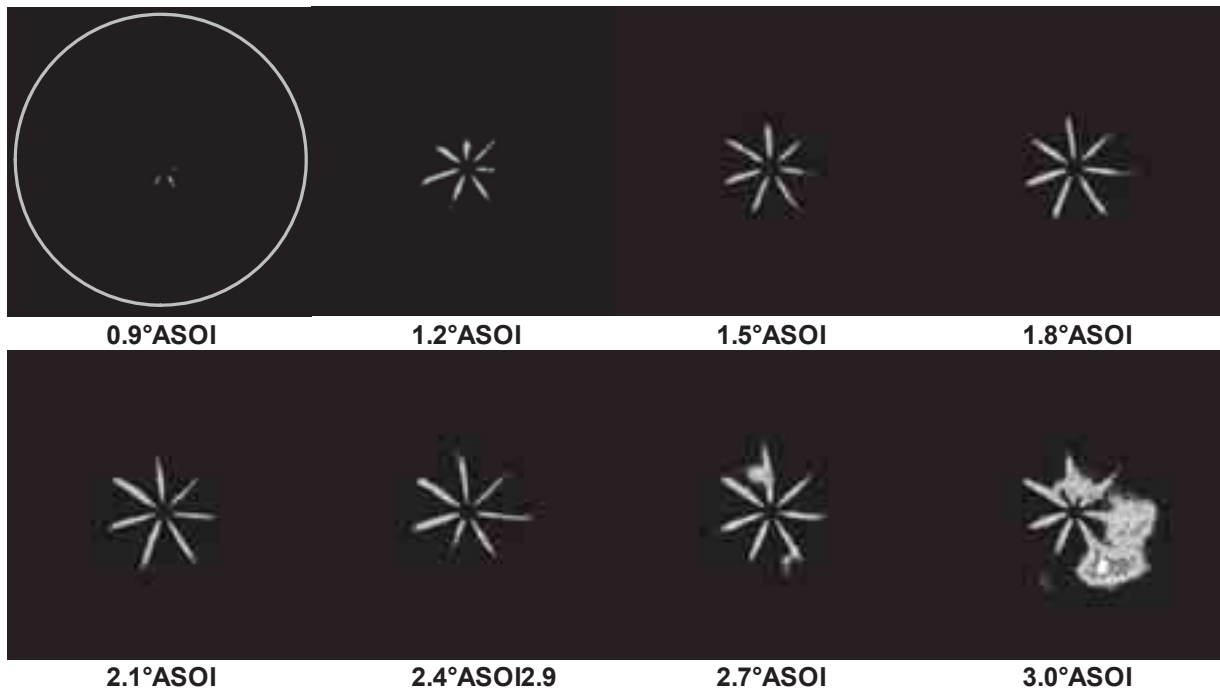


Fig. 4. Spray evolution from the start of injection until autoignition for diesel fuel (SOI= 1 CAD ATDC, EGR=0%)

Figures 5-6 show the effects of tested fuels on the first stages of the combustion process after the autoignition. For each selected sequence, the flame went up the direction of the spray axis, following the stoichiometric air-fuel ratio path. Due to the strong swirl, the flame, previously induced, spread in the combustion chamber dragged by the anticlockwise air motion. For all the conditions the ignition delay measured by luminous signal was in agreement with that measured by pressure related data. In early injection condition (11 CAD BTDC) the flame spread in the combustion chamber faster than other SOI; this effect determined fast increase in temperature and pressure of the combustion chamber and it was directly correlated to the high concentration of nitrogen oxides measured at the exhaust.

The auto ignition attended together the spray evolution for all conditions and fuels until the SOI=5 CAD ATDC. At this injection timing, diesel fuel jets resulted well resolvable for both the EGR rates. On the contrary, for G20 and BU20 the whole amount of fuel is injected before the start of combustion when the engine worked with high EGR rate. This demonstrated how the premixed low temperature regime (PLTC) was achieved for both diesel blends. Due to the higher ignition delay, BU20 induced a PLTC mechanism in wider range of conditions compared to G20.

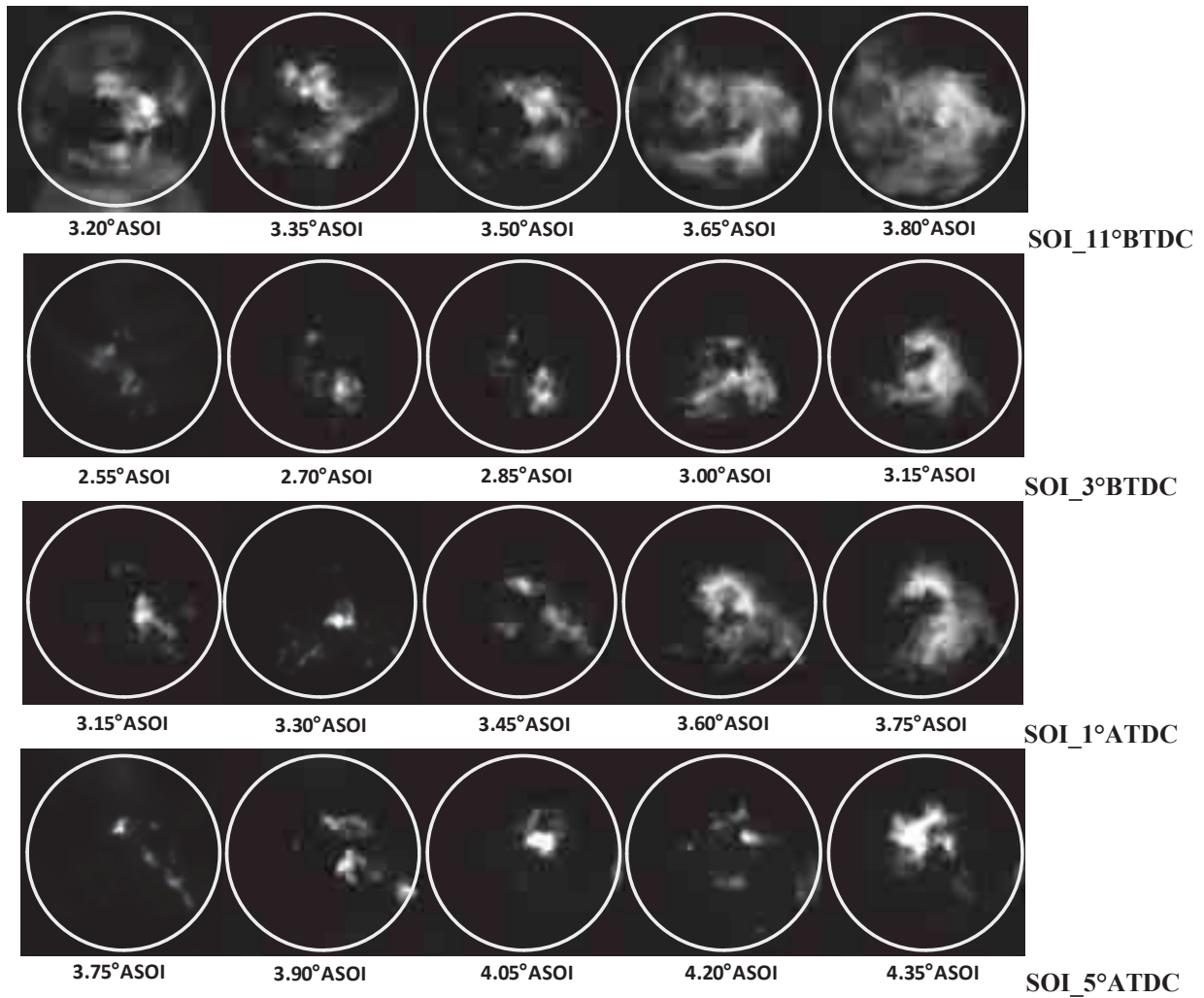


Fig. 5. UV-VIS flame emission measured for Diesel. Injection occurred at different SOI and without EGR

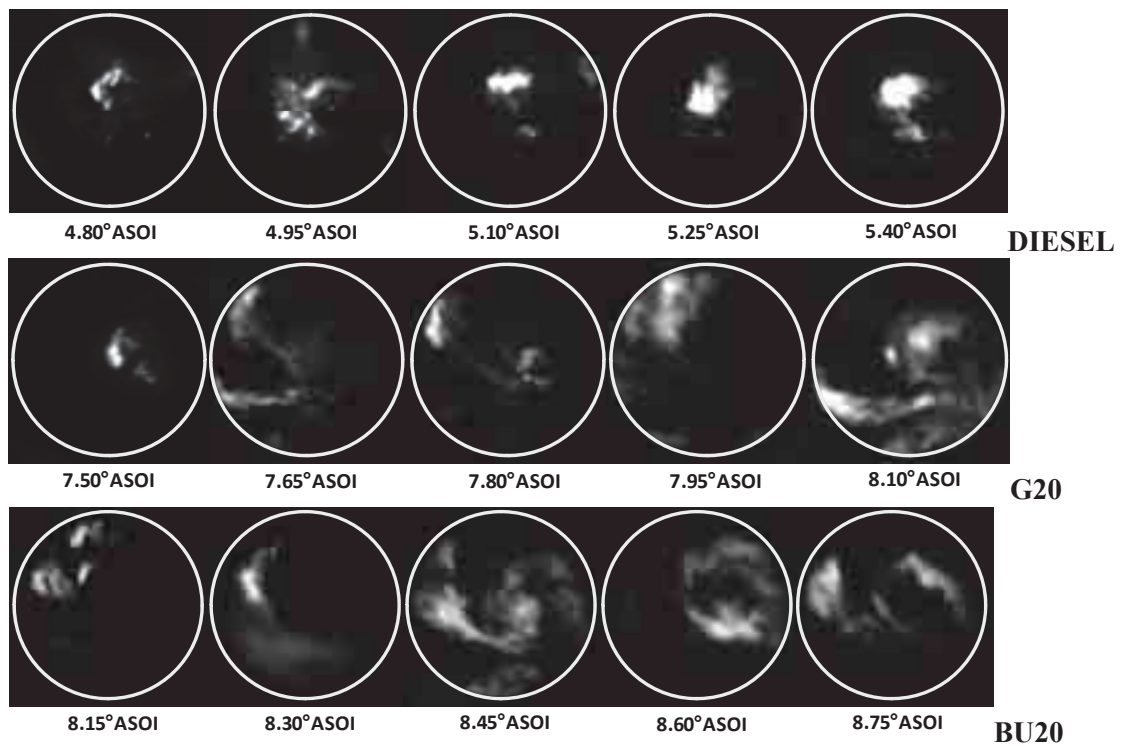


Fig. 6. UV-VIS flame emission for Diesel, G20 and BU20 fuel, SOI=5 CAD ATDC (50%EGR)

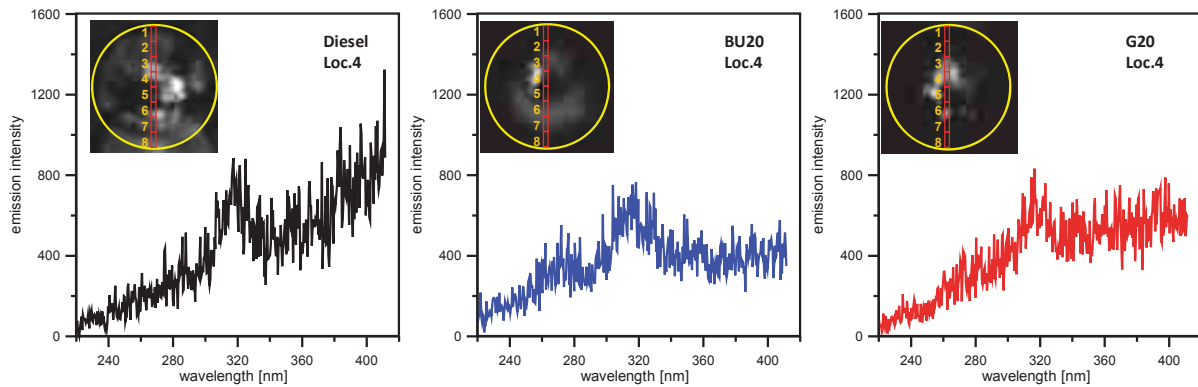


Fig. 7. UV emission spectra detected at 0.5 CAD ASOC in central location of the combustion chamber (SOI=11 CAD BTDC, EGR%=0)

In order to follow the evolution of the chemical species that are markers of the combustion process, natural emission spectroscopy measurements were performed. Fig. 7 show typical spectra detected at 0.5 CAD ($\sim 166 \mu\text{s}$) after the auto-ignition in central location (Loc. 4) of the combustion chamber for the condition with SOI=11 CAD BTDC and EGR%=0. Similar spectral behaviour was observed for the different fuels. The two OH emission bands in the range 305-320 nm and 270-280 nm were well resolved. The first band systems were due to the diagonal OH(0,0) and OH(1,1) transitions of $A^2 \Sigma^+ - X^2 \Pi_i$; the second one was related to the off-diagonal OH(1,0) transitions [6, 7]. The weak emission of CH band system near 390 nm was detected only for diesel fuel. The CH band around 314 nm cannot be resolved because it is very weak with closely packed heads and is obscured by OH. OH and CH features were superimposed on a broadband emission due to two band systems. The first bands were due to the Emeleus' bands of formaldehyde molecule CH_2O and it had the highest emission in the range from 350 nm to 460 nm. The second emission system identified the Vaidya's bands of HCO with highest heads from 290 nm to 360 nm [8]. It should be noted that for BU20 and G20 the HCO+ CH_2O band intensities were inversely correlated to the off-diagonal OH emissions, due to higher oxygen and hydrogen mass fraction of butanol than gasoline. For diesel fuel the weak CH evidence is related to an emission signal that increase with the wavelength. This result is due to PAH and soot precursors formed in the combustion chamber.

The flame spread fast in the combustion chamber and it occurred less than 1 CAD to observe a strong soot emission in the centre of the combustion chamber (Fig. 8). Soot was characterized by a broadband feature that increased with the wavelength like a blackbody curve [9, 10]. For G20 the OH formed in the first combustion stages persisted at the inception of soot formation reducing its effect. During the combustion process the spectra corresponding at same injection timing evolved with the same spectral features until the start of oxidation phase when the soot emission decreased and OH band system came out demonstrating OH radical as one of the principal markers of the soot oxidation [11]. The effect is well observed in Fig. 9 that shows the spectra detected at 10 CAD ASOI for the condition SOI=11 CAD BTDC, EGR%=0.

Spectroscopic data retrieved using the procedure described in previous paragraph, allowed to follow the time-evolution of soot and OH. Results obtained for the conditions with SOI = 11 CAD BTDC and 3 CAD BTDC are reported in Fig. 10 and 11. For all the tests, EGR resulted more effective for G20 and BU20 than diesel, inducing higher difference in the formation rate and maximum value. Around 10 CAD ATDC, the combustion chamber flow moved towards the exhaust. At this time soot emission of diesel resulted higher than blends for all the conditions while OH was higher. PPLTC regime drastically reduced the OH and soot emission and at 10 CAD ATDC soot reached the limit of the optical detection. Optical data related to the combustion chamber agree with the smoke-NO_x value measured at the exhaust.

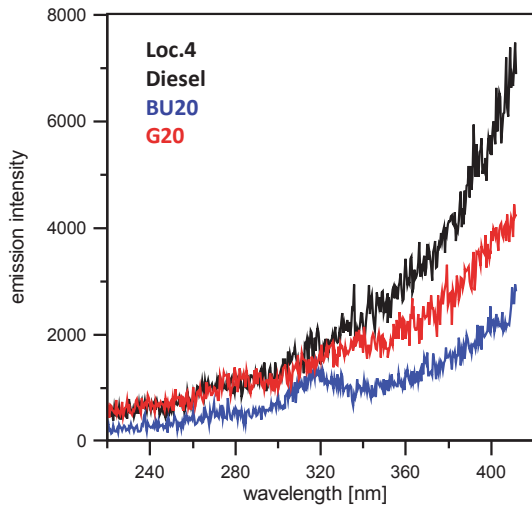


Fig. 8. UV emission spectra detected at 0.8 CAD ASOC in central location of the combustion chamber (SOI=11 CAD BTDC, EGR%=0)

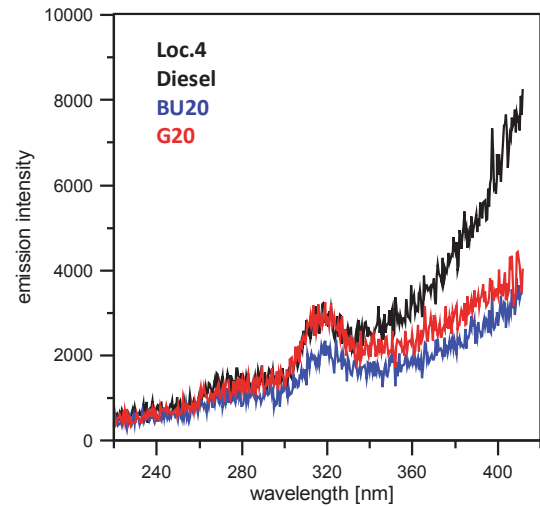


Fig. 9. UV emission spectra detected at 10 CAD ASOC in central location of the combustion chamber (SOI=11 CAD BTDC, EGR%=0)

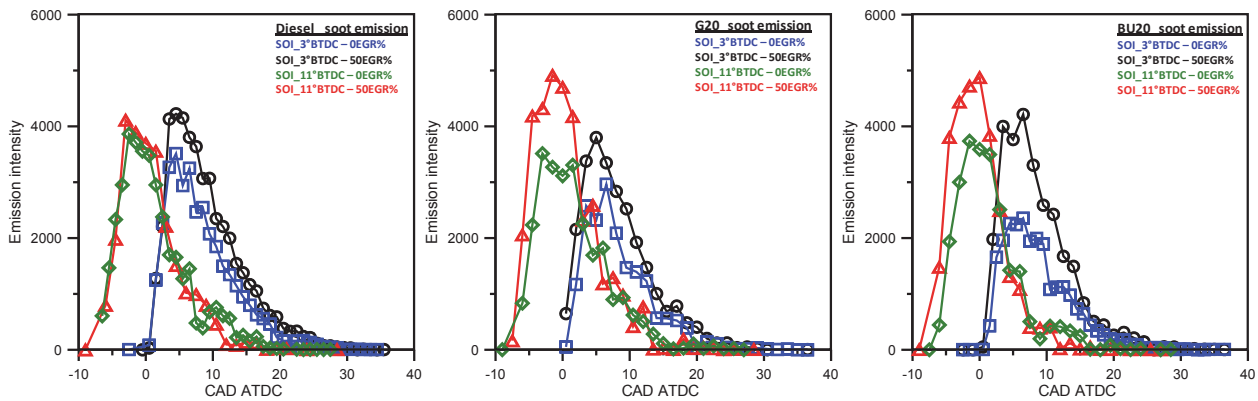


Fig. 10. Soot evolution evaluated from spectroscopic measurements for the conditions with SOI = 11 CAD BTDC and 3 CAD BTDC

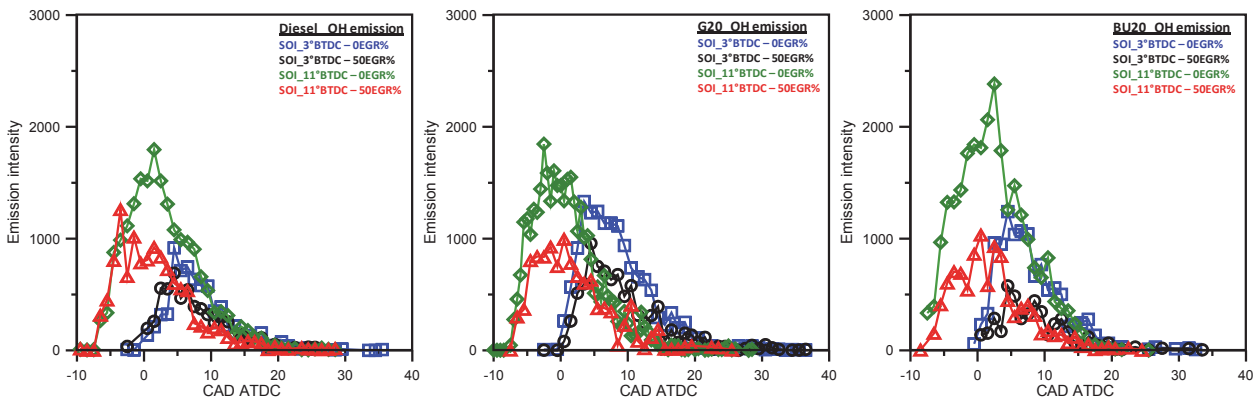


Fig. 11. OH evolution evaluated from spectroscopic measurements for the conditions with SOI = 11 CAD BTDC and 3 CAD BTDC

4. Conclusions

UV-visible digital imaging and natural emission spectroscopy were applied in a single cylinder optically accessible high swirl multi-jets compression ignition engine to investigate spray combustion process in several engine conditions. Commercial diesel fuel, pure and blended with butanol (BU20) and gasoline (G20), was tested. The blends allowed to reduce the cetane number

with respect to diesel. Injection timings and EGR rate were changed in order to achieve three combustion modes: conventional diesel combustion, mixing controlled combustion and partially premixed low-temperature combustion. The last one was reached only for the blends with late injection and 50%EGR. The two advanced combustion modes (MCC and PPLTC) showed low smoke and NO_x emission at the exhaust. MCC resulted more efficient and with higher stability than low temperature regime.

Optical investigations demonstrated that fixing the fuel injection strategy, the fuel composition principally influenced the rate of soot formation and oxidation rather than highest value. This occurred thanks to higher and faster production of OH radicals.

Acknowledgements

The authors would like to express their sincere appreciation to Mr. A. Mazzei for the technical support in preparing the equipment and during the experiments.

References

- [1] Zhao, H., Ladommatos, N., *Optical diagnostics for in-cylinder mixture formation measurements in IC engines*, Progress in Energy and Combustion Science, 24 (4), pp. 297–336, 1998.
- [2] Splitter, D. A., Hanson, R., Kokjohn, S., Rein, K., Sanders, S., Reitz, R. D., *An Optical Investigation of Ignition Processes in Fuel Reactivity Controlled PCCI Combustion*, SAE paper 2010-01-0345, 2010.
- [3] Delacourt, E., Desmet, B., Besson, B., *Characterisation of very high pressure diesel sprays using digital imaging techniques*, Fuel, 85, pp. 859–867, 2005.
- [4] Soida, S. N., Zainal, Z. A., *Spray and combustion characterization for internal combustion engines using optical measuring techniques – A review*, Energy, 36(2), pp. 724–741, 2011.
- [5] Jin, C., Yao, M., Liu, H., Lee, C. F., Ji, J., *Progress in the production and application of n-butanol as a biofuel*, Renewable and Sustainable Energy Reviews, 15(8), pp. 4080-4106, 2011.
- [6] Copeland, R. A., Jeffries, J. B., Crosley, D. R., *Transition probabilities in OH $A^2\Sigma^+ - X^2\Pi_i$ bands with $v' = 0$ and 1 , $v'' = 0$ to 4* , Chemical Physics Letters, 138(5), pp. 425-430, 31 July 1987.
- [7] Crosley, D. R., Lengel, R. K., *Relative transition probabilities and the electronic transition moment in the A-X system of OH*, J. Quant. Spectrosc. Radiat. Transfer 15, pp. 579–591, 1975.
- [8] Gaydon, A. G., Wolfhard, H. G., *Mechanism of formation of CH, C₂, OH and HCO radicals in flames*, Symposium (International) on Combustion, 4(1), pp. 211-218, 1953.
- [9] Zhao, H., Ladommatos, N., *Optical diagnostics for soot and temperature measurement in diesel engines*, Progress in Energy and Combustion Science 24(3), pp. 221-255, 1998.
- [10] Senda, J., Choi, D., Iwamuro, M., Fujimoto, H. et al., *Experimental Analysis on Soot Formation Process In DI Diesel Combustion Chamber by Use of Optical Diagnostics*, SAE Technical Paper n.2002-01-0893, 2002.
- [11] Nagle, J., Strickland-Constable, R. F., *Oxidation of Carbon Between 1000°-2000°C*, Proc. 5th Conf. on Carbon – Pergamon, 1961.